Activation of persulfate by Fe(III) species: Implications for 4-tert-butylphenol degradation

Yanlin Wu, Romain Prulho, Marcello Brigante, Wenbo Dong, Khalil Hanna, Gilles Mailhot

Activation of persulfate by Fe(III) species: Implications for 4-tert-butylphenol degradation

Yanlin Wu[a,b,c,d], Romain Prulho[a,b], Marcello Brigante[a,b*], Wenbo Dong[e], Khalil Hanna[c*], Gilles Mailhot[a,b]

[a] Université Clermont Auvergne, Université Blaise Pascal, Institut de Chimie de Clermont-Ferrand, BP 10448, F-63000 Clermont-Ferrand, France

[b] CNRS, UMR 6296, ICCF, F-63171 Aubière, France

[c] Ecole Nationale Supérieure de Chimie de Rennes UMR CNRS 6226, 11 Allée de Beaulieu, CS 50837, F-35708 RENNES Cedex 7, France

[d] State Key Laboratory of Pollution Control and Resources Reuse, College of Environmental Science and Engineering, Tongji University, Shanghai 200092, China

[e] Shanghai Key Laboratory of Atmospheric Particle Pollution and Prevention, Department of Environmental Science and Engineering, Fudan University, Shanghai 200433, China

***Corresponding authors**: marcello.brigante@univ-bpclermont.fr ;*

khalil.hanna@ensc-rennes.fr

Highlights

- A new AOPs method based on iron oxide activation of persulfate.
- Radical species involvement during persulfate activation was investigated.
- Effect of naturally occurring scavengers such as carbonates and chloride ions was assessed.

Abstract

In this study, the activation of persulfate induced by Fe(III) species, including 5 kinds of iron oxhydroxides (IOs) and dissolved Fe^{3+} under dark condition were investigated. Ferrihydrite (FH) and akaganeite (AK) showed the highest activity in 4-tert-butylphenol (4tBP) removal. The 4tBP degradation rate constant decreased as the solution pH increased from pH 3.2 to 7.8 in FH/$S_2O_8^{2-}$ system. However, the pH value had no significant effect on the 4tBP degradation in AK/$S_2O_8^{2-}$

system. The degradation of 4tBP in $Fe^{3+}/S_2O_8^{2-}$ system was also performed to investigate the role of ferric species in persulfate activation. The pH dependency of 4tBP degradation rate was closely related to the speciation of Fe^{III}, whereas the $Fe(H_2O)_6^{3+}$ was found to be the most active soluble iron complex form in the activation of $S_2O_8^{2-}$. 4tBP degradation was mainly due to the $SO_4^{\bullet-}$ in $IOs/S_2O_8^{2-}$ system, while $SO_4^{\bullet-}$ and $HO_2^{\bullet}$ both had great contribution on 4tBP degradation in $Fe^{3+}/S_2O_8^{2-}$ system. Further investigations showed clearly that 4tBP degradation efficiency was decreased significantly due to the trapping of $SO_4^{\bullet-}$ by chloride. This finding may have promising implications in developing a new technology for the treatment of contaminated waters and soils, especially where Fe^{3+} species are naturally occurring.

1. Introduction

Persulfate has received increasing interest in recent years in the application for the degradation of organic pollutants in contaminated soils and waters. Persulfate anion ($S_2O_8^{2-}$) is usually activated by thermal [1, 2], alkaline [3], ultraviolet light [4-6] or transition metal (Fe^0, Fe^{2+}, Cu^{2+}, Co^{2+} and Ag^+) [7-9] to form sulfate radical ($SO_4^{\bullet-}$), which has high oxidation-reduction potential (E^o = 2.6 - 3.2 V) [10, 11]. It could be an alternative to traditional advanced oxidation processes (AOPs) which are based on hydroxyl radical ($HO^{\bullet}$) generation, such as Fenton or Fenton-like oxidation. In fact, $SO_4^{\bullet-}$ have the potential for much greater stability than $HO^{\bullet}$ and wide reactivity like $HO^{\bullet}$ and so could be very efficient for the treatment of wastewaters containing high concentrations of organic contaminants [12, 13].

One of the most common activators of persulfate (PS) includes soluble iron and iron chelates [8, 14, 15]. Activation of persulfate by iron or other transition metals proceeds through reduction of persulfate to generate $SO_4^{\bullet-}$ which is a reaction parallel to the Fenton initiation reaction [16, 17]:

$$S_2O_8^{2-} + Fe^{2+} \rightarrow Fe^{3+} + SO_4^{2-} + SO_4^{\bullet-} \qquad (k = 27\ M^{-1}\ s^{-1}) \qquad (R1)$$

Homogeneous processes with soluble iron have been widely investigated to produce radical species and remove non-biodegradable compounds, but pH should be lowered to around 4 to avoid iron precipitation [18-20]. In order to overcome this limitation, minerals could be used to promote the oxidation reaction at circumneutral pH [14, 21,

22].

Recently, number of research works have studied the use of transition metal (Cu, Fe and Mn)-bearing minerals to catalyze the decomposition of persulfate and degrade organic compounds in waters [14, 21-28]. However, persulfate activation mechanism at oxide surfaces and generation pathways of reactive oxygen species (e.g. $HO^{\bullet}$, $SO_4^{\bullet-}$, $O_2^{\bullet-}$) are still a matter of debate. While the most of these works indicated the radical formation (at surface or in solution) as the main mechanism responsible of contaminant removal [24-27, 29, 30], Zhang et al. reported that copper oxide can efficiently activate $S_2O_8^{2-}$ without producing sulfate radicals [27]. Indeed, the activation mechanism and radical generation strongly depends on the activator surface active sites, surface composition and charge transfer processes [24-26, 29, 30]. More particularly, Liu et coworkers [29, 31] demonstrated that Fe(III)-oxides such as goethite were able to catalytically convert persulfate into sulfate radical ($SO_4^{\bullet-}$) and hydroxyl radical ($HO^{\bullet}$), but by using an high mineral mass loading ($\geq$ 50 g L^{-1}) and at pH 8 maintained with 50 mM borate buffer. Therefore, more investigations are still needed to determine the role of Fe(III) species in persulfate activation and radical generation under different chemical conditions.

In the present work, the ability of five selected iron oxhydroxides in PS activation was investigated under different experimental conditions (pH value, solid concentration and $S_2O_8^{2-}$ concentration). To provide insights into the role of ferric species in persulfate activation, experiments were also conducted with the dissolved Fe(III) (Fe^{3+} ion added as $Fe(ClO_4)_3$). The speciation of the latter is most important in aqueous solution and dominated by the hydrolysis and then subsequent formation of different Fe^{III} complexes as the pH increases [32].

4-tert-butylphenol (4tBP), an emerging contaminant, was used as a target pollutant, which is one of the endocrine disrupting chemicals with highly estrogenic effects [33, 34]. 4tBP had been widely used as a raw material for chemical industry [35], and thus found at relatively high concentrations in aquatic and environmental systems [36]. The effects of chloride (Cl^-) and carbonates (HCO_3^-/CO_3^{2-}) ions, which are considered as the most naturally occurring anions, on the transformation of 4tBP

were experimentally investigated. The identification of the main reactive oxygen species in Fe(III)/persulfate system was also performed by conducting radical quenching experiments.

2. Experimental

2.1. Chemical

Potassium persulfate ($K_2S_2O_8$), 4-tert-butylphenol (4tBP) and Ferric perchlorate ($Fe(ClO_4)_3$) 2-Propanol (2-Pr) and tert-Butanol (t-BuOH) were obtained from Sigma-Aldrich, France and used without further purification. Perchloric acid ($HClO_4$) (that is not reactive toward photogenerated radicals [37]) and sodium hydroxide (NaOH) were used to adjust the pH of the solutions. All chemicals were used without further purification. Hematite, Goethite, Lepidocrocite, Ferrihydrite and Akaganeite were synthesized as explained in previous works [38-40]. The obtained particles were characterized for particle size and B.E.T. specific surface area N_2(g) adsorption measurements, chemical analysis, transmission electron microscopy (TEM) and X-ray diffraction (XRD). Their main characteristics are summarized in Table 1.

2.2. Experimental procedure

All the experiments were carried out in brown reaction flask, to avoid any light irradiation, with constant magnetic stirring at room temperature (293 ± 2 K). The initial concentration of 4tBP was 50 μM in all experiments. The pH value was measured by Cyberscan 510 pH meter. Samples were taken from the reaction flask at fixed time period and they were passed through the filter (0.22 μm) before chromatographic analysis.

2.3. Chemical species quantification

The concentration of the 4tBP remaining in the aqueous solution was determined by high performance liquid chromatography (HPLC) equipped with a photodiode array detector (Waters 996, USA), an HPLC pump (Waters 515, USA) and an auto-sampler (Waters 717, USA). The experiments were performed by UV detection at 221 nm. The flow rate was 1 mL min^{-1} and the mobile phase was a mixture of water

and methanol (20/80, v/v). The column was a Zorbax RX-C8 of 250 mm × 4.6 mm × 5 μm. Under these conditions, the retention time of 4tBP was 6.5 min.

To measure the aqueous concentration of total iron at the end of the experiment, aliquots were sampled from the flasks, filtered through 0.22 μm filters and added to a tube that contained 0.5 N ascorbic acid which reduced all of the dissolved iron into Fe(II). The total Fe(II) in a given solution was determined colorimetrically by the ferrozine assay as previously reported in Bianco et al. [41].

The scavenging experiments were performed using 2-Pr and t-BuOH to determine the contributions of $SO_4^{\bullet-}$ and $HO^{\bullet}$ for the degradation of 4tBP.

3. Results and discussion

3.1. Degradation kinetic of 4tBP in unbuffered systems

The degradation kinetics of 4tBP in the presence of iron oxhydroxides (IO)/ persulfate (PS) and in unbuffered solution are shown in Figure 1. The initial pH was 4.7 without pH adjustment and the value was found stable within ± 0.2 pH unit during the reaction. Very low adsorption of 4tBP was observed whatever the tested solid (0.9%, 0.5%, 1.0%, 0.9% and 1.0% respectively for Hematite, Goethite, Lepidocrocite, Ferrihydrite and Akaganeite under adopted experimental conditions).

. A slight degradation (less than 3%) was observed in IO-free system after 6 h of reaction, while the presence of IOs enhanced the 4tBP degradation efficiency regardless of the IO tested. Among the tested IOs, ferrihydrite (FH) and akaganeite (AK) showed the highest performance in 4tBP removal. However, it should be noted that amount of dissolved iron (Fe(II/III)) was found below the detection limit (corresponding to 1 μM) whatever the investigated system.

The degradation rate constants of 4tBP (k_{4tBP}, s^{-1}) are then evaluated at different amounts of FH and AK (Figure 2). As expected, the removal efficiency increased with the increasing solid concentration in both AK/$S_2O_8^{2-}$ and FH/$S_2O_8^{2-}$ systems. In particular, increasing of AK concentration had more pronounced effect on 4tBP degradation than that of FH. Indeed, the degradation rate constant increased rapidly

from 3.0×10^{-6} s^{-1} to 3.0×10^{-4} s^{-1} as the concentration of AK increased from 2.4 m^2 L^{-1} to 239 m^2 L^{-1}.

In the Fenton system, the surface reactivity of each type of mineral is likely affected by crystallinity, surface composition and metal coordination [29, 42]. It is generally admitted that the degradation rate was much higher in the presence of amorphous oxides than crystalline ones [42, 43]. For instance, ferrihydrite (i.e. the least crystallized iron oxyhydroxide) showed higher efficiency than crystallized oxides (e.g. goethite, lepidocrocite and hematite) in heterogeneous Fenton reaction [29, 42]. In the present study, AK (β-FeOOH) exhibited, however, higher rate constants than FH. Moreover, only heterogeneous surface reaction occurred, since the amount of dissolved iron was negligible (below the detection limit) regardless of the solid loading.

3.2. Effect of pH and investigations of reaction mechanism

Figure 3 shows the variation of 4tBP degradation rate constant in the presence of FH and AK within the pH range between 3.2 and 7.8. While no significant effect of pH value on the 4tBP degradation in AK/$S_2O_8^{2-}$ system was noted, the degradation rate constant in FH/$S_2O_8^{2-}$ system decreased from 3.2×10^{-5} s^{-1} to 1.1×10^{-5} s^{-1} as the solution pH increased from pH 3.2 to 7.8. Almost no leaching of iron ions can be detected at all pH values as the total iron concentration was below the detection limit, < 1 µM, even in acidic conditions. While the pH effect in FH system was quite expected, an unusual trend was observed for AK. This may be explained both by the higher isoelectric point/point-of-zero charge (PZC) (9.6 − 10) of this mineral than of FH (~ 8), and an additional surface complexation mechanism at the (010) plane. Geminal sites (≡$Fe(OH)_2^{2+}$) at this plane could be especially reactive for metal-bonded complexes, as they facilitate a mononuclear six-membered chelate complex via the displacement of two hydroxo/aquo groups at the equatorial plane of a single Fe octahedron. This explanation has been recently used to explain why the AK has a higher sorption capacity for organic ligands as a function of pH than other Fe(III) oxhydroxides [44].

The electrostatic interactions between oxide surfaces and 4tBP (p*K*a ~9.8) should be ignored in the pH range investigated (3.2 - 7.8), as the PZC of the FH or AK are higher than 8 (Table 1). In addition, PS is under anionic form whatever the pH tested, and should interact with a positively charged iron oxhydroxides due to the electrostatic attraction between the oxide surface and PS. So, interactions between protonated 4tBP and negatively charged $S_2O_8^{2-}$ species adsorbed on positively charged oxide surfaces may be favorable in the case of AK. Previous investigations showed a strong inverse pH-dependency of the degradation rate on CuO or Fe_3O_4 systems [25]. The authors have suggested a different degradation pathway related with pH of medium and to the adverse impact of pH on PS activation where H^+ would probably form an H-bond with the negatively charged oxygen in the $S_2O_8^{2-}$ molecule and thus inhibit its interaction with positively charged surface.

By analogy to the Fenton-like system [42], Liu et al. [29] have proposed an one-electron reduction of ≡Fe(III) surface site, which result in the formation of persulfate radical ($S_2O_8^{\bullet-}$).

$$\equiv Fe^{III}OH + S_2O_8^{2-} \rightarrow \equiv Fe^{II}OH + S_2O_8^{\bullet-} \quad \text{(R2)}$$

$S_2O_8^{\bullet-}$ can be involved in radical chain reactions with water [29, 31], while freshly generated Fe^{II} react with $S_2O_8^{2-}$ to generate radical sulfate $SO_4^{\bullet-}$ through the following reaction:

$$\equiv Fe^{II}OH + S_2O_8^{2-} \rightarrow \equiv Fe^{III}OH + SO_4^{2-} + SO_4^{\bullet-} \quad \text{(R3)}$$

$SO_4^{\bullet-}$ can also react with water or OH^- to generate $HO^\bullet$ [31].

$$SO_4^{\bullet-} + H_2O \rightarrow SO_4^{2-} + HO^\bullet + H^+ \quad \text{(R4)}$$

$$SO_4^{\bullet-} + HO^- \rightarrow SO_4^{2-} + HO^\bullet \quad \text{(R5)}$$

$SO_4^{\bullet-}$ or $HO^\bullet$ can react with persulfate to generate additional $S_2O_8^{\bullet-}$:

$$SO_4^{\bullet-} + S_2O_8^{2-} \rightarrow SO_4^{2-} + S_2O_8^{\bullet-} \quad \text{(R6)}$$

$$HO^\bullet + S_2O_8^{2-} \rightarrow HO^- + S_2O_8^{\bullet-} \quad \text{(R7)}$$

Formation of $S_2O_8^{\bullet-}$ form oxidation $S_2O_8^{2-}$ via a one-electron transfer reaction was also previously reported [45, 46].

Experiments were then conducted with dissolved ferric iron concentration at 11.2 mM at pH 2.4. At this iron concentration and pH, ferric ions were present under monomeric ferric aquacomplex forms ($Fe(H_2O)_6^{3+}$ and $Fe(H_2O)_5(OH)^{2+}$) [47].

The degradation of 4tBP in Fe(III)/$S_2O_8^{2-}$ system was performed at different pH values (2.4 - 5.0 where all the Fe(III) amount is under dissolved form) (figure 4). The control experiments (4tBP/Fe(III) and 4tBP/$S_2O_8^{2-}$) were performed at pH 2.4 and less than 4% of 4tBP degradation was observed. The results showed that the degradation rate of 4tBP is strongly dependent on pH, i.e. slight decrease in the range 2.4 to 2.7 following by a sharp fall at pH > 2.7 before reaching zero at pH 5.0. This pH dependency is closely related to the speciation of Fe^{III}, and thus the different forms of iron aqua-complexes ($Fe(H_2O)_6^{3+}$, $Fe(H_2O)_5(OH)^{2+}$, $Fe(H_2O)_4(OH)_2^{+}$) existing between pH 1 and 5 ([47] and Figure SM1). These complexes may have different reactivities with $S_2O_8^{2-}$. It is worth noting that the percentage of $Fe(H_2O)_6^{3+}$ species and the 4tBP degradation rate exhibited similar trend as a function of pH, suggesting a significant contribution of this complex in the activation of $S_2O_8^{2-}$.

To confirm the crucial role of $Fe(H_2O)_6^{3+}$ form, the impact of soluble Fe(III) concentration was tested at pH 2.4 (Figure 5). The percentage of the form $Fe(H_2O)_6^{3+}$ is around 60% whatever the Fe(III) concentration used in our experimental conditions. The degradation rate constant increased rapidly from 7.6×10^{-5} s^{-1} to 7.5×10^{-4} s^{-1} as the concentration of Fe(III) increased from 1.12 mM to 11.2 mM corresponding to the increase of $Fe(H_2O)_6^{3+}$ amount from 0.67 mM to 6.7 mM. These results confirm the significant role of Fe^{3+} for the activation of persulfate, and more specifically the role of the aqueous complex $Fe(H_2O)_6^{3+}$.

3.3. Identification of involved radicals at pH 2.4

To determine the nature of involved radicals during the degradation of 4tBP, experiments were conducted with 50 mM of 2-Pr or t-BuOH. At adopted concentrations, 2-Pr was considered to quench efficiently both generated $SO_4^{\bullet-}$ and

$HO^{\bullet}$ considering the second order rate constants of $k_{2-Pr,SO_4^{\bullet-}}$ = 7.42 × 10^7 M^{-1} s^{-1} and $k_{2-Pr,HO^{\bullet}}$ = 1.9 × 10^9 M^{-1} s^{-1}, while t-BuOH can be considered to be more selective toward $HO^{\bullet}$ ($k_{t-ButOH,HO^{\bullet}}$ = 6.0 × 10^8 M^{-1} s^{-1}) than $SO_4^{\bullet-}$ ($k_{t-ButOH,SO_4^{\bullet-}}$ = 8.31 × 10^5 M^{-1} s^{-1}) [48, 49]. It is then possible to estimate the radical scavenging percentage by using the aqueous concentration of each chemical and the reactivity of radicals with 4tBP ($k_{4tBP,HO^{\bullet}}$ = 1.6 × 10^{10} M^{-1} s^{-1} and $k_{4tBP,SO_4^{\bullet-}}$ = 4.2 × 10^9 M^{-1} s^{-1} [50]). About 99% of $HO^{\bullet}$ and 95% of $SO_4^{\bullet-}$ would be quenched in the presence of 2-Pr (50 mM), while in the presence of t-BuOH (50 mM) the values can be estimated to be about 97% of $HO^{\bullet}$ and 20% of $SO_4^{\bullet-}$. We can argue that the difference observed in 4tBP degradation when the scavengers were used separately should correspond to the contribution of $SO_4^{\bullet-}$.

In both FH/$S_2O_8^{2-}$ and AK/$S_2O_8^{2-}$ systems, 4tBP degradation was completely inhibited in the presence of 2-Pr, while the inhibition of 4tBP degradation was insignificant using t-BuOH (Figure 6). This trend suggests that $SO_4^{\bullet-}$ is mainly responsible for the 4tBP degradation in our experimental conditions. More precisely, 91% of $SO_4^{\bullet-}$ and 9% of $HO^{\bullet}$ are involved in FH/$S_2O_8^{2-}$ system, whereas 94% of $SO_4^{\bullet-}$ and 5.5% of $HO^{\bullet}$ in AK/$S_2O_8^{2-}$ system.

Around 43% of degradation of 4tBP was still observed in the presence of 2-Pr in Fe(III)/$S_2O_8^{2-}$ system, suggesting the occurrence of additional oxidant species. Addition of benzoquinone (BQ) in Fe(III)/$S_2O_8^{2-}$ system completely inhibited the degradation of 4tBP in the presence of 2-Pr. It is well known that BQ is an electron acceptor able to interrupt dissolved oxygen accepting electrons, and so acts as a very effective trap to avoid the formation of hydroperoxyle radical/superoxide radical anion ($HO_2^{\bullet}$/$O_2^{\bullet-}$) [51, 52]. It is, therefore, reasonable that $HO_2^{\bullet}$ can be formed in our experimental conditions (pH = 2.4 < pKa($HO_2^{\bullet}/O_2^{\bullet-}$) , as shown in R8-R10 [53].

$$Fe(H_2O)_6^{3+} + S_2O_8^{2-} \rightarrow Fe(H_2O)_6^{2+} + S_2O_8^{\bullet-} \qquad \text{(R8)}$$

$$Fe(H_2O)_6^{2+} + S_2O_8^{2-} \rightarrow SO_4^{\bullet-} + SO_4^{2-} + Fe(H_2O)_6^{3+} \qquad \text{(R9)}$$

$$Fe(H_2O)_6^{2+} + O_2 \rightarrow O_2^{\bullet-} + Fe(H_2O)_6^{3+} \quad \text{(R10)}$$

The relative contributions of $SO_4^{\bullet-}$, $HO^{\bullet}$ and couple $HO_2^{\bullet}$/ $O_2^{\bullet-}$ (pKa ~ 4.9) to the degradation of 4tBP were then estimated as 55%, 1% and 44% respectively, in Fe(III)/$S_2O_8^{2-}$ system.

3.4. Effect of chloride and carbonates anions

To evaluate the impact of naturally occurring inorganic ions, experiments were conducted with FH or AK at pH = 4.7 in the presence of chloride ions (Cl^-). As shown in Figure 7, addition of Cl^- (0.1 and 0.5 M) strongly inhibited the 4tBP degradation in all investigated systems.

The inhibition of 4tBP degradation can be attributed to the quenching of $SO_4^{\bullet-}$ by chloride ions. In fact, Cl^- reacts with $SO_4^{\bullet-}$ to generate $Cl^{\bullet}$ (R11) which rapidly combines with another chloride ion in water forming dichloride radical anion ($Cl_2^{\bullet-}$) (R12) .

$$SO_4^{\bullet-} + Cl^- \rightarrow Cl^{\bullet} + SO_4^{2-} \qquad k_{SO_4^{\bullet-},Cl^-} = 2.0 \times 10^8\ M^{-1}\ s^{-1}\ [49] \quad \text{(R11)}$$

$$Cl^{\bullet} + Cl^- \rightarrow Cl_2^{\bullet-} \qquad k_{Cl^{\bullet},Cl^-} = 0.8 - 2.1 \times 10^{10}\ M^{-1}\ s^{-1}\ [54, 55] \quad \text{(R12)}$$

The reducing potential of $Cl_2^{\bullet-}$ (E^o = 2.09 V) is lower than $SO_4^{\bullet-}$ (E^o = 2.6-3.2 V). Additionally, the second order rate constants of 4tBP with $SO_4^{\bullet-}$ ($k_{4tBP,SO_4^{\bullet-}}$ = 4.2 × 10^9 M^{-1} s^{-1}) and $Cl_2^{\bullet-}$ ($k_{4tBP,Cl_2^{\bullet-}}$ = 2.78 × 10^8 M^{-1} s^{-1}) estimated by laser flash photolysis following previously reported approach [56] indicated that the formed $Cl_2^{\bullet-}$ had lower reactivity for 4tBP oxidation than $SO_4^{\bullet-}$ (more than 10 times). The addition of carbonates (2 and 10 mM) at pH 8.2 (corresponding to 98% in the form of HCO_3^-) completely inhibited the 4tBP degradation. In fact, carbonates are able to quench $SO_4^{\bullet-}$ via reactions R13 and R14 to generate the carbonate radical ($CO_3^{\bullet-}$)[49], which is less oxidant than $SO_4^{\bullet-}$ [57]. This is in agreement with previous reports where scavenging effects of chloride and carbonates anions towards $SO_4^{\bullet-}$ radicals were observed [58, 59].

$$SO_4^{\bullet -} + HCO_3^- \rightarrow CO_3^{\bullet -} + H^+ + SO_4^{2-} \qquad k_{SO_4^{\bullet -}, HCO_3^-} = 9.1 \times 10^6\ M^{-1}\ s^{-1} \qquad (R13)$$

$$SO_4^{\bullet -} + CO_3^{2-} \rightarrow CO_3^{\bullet -} + SO_4^{2-} \qquad k_{SO_4^{\bullet -}, CO_3^{2-}} = 4.1 \times 10^6\ M^{-1}\ s^{-1} \qquad (R14)$$

4. Conclusions

We have demonstrated that the persulfate could be activated by Fe(III) species, including iron oxhydroxides and dissolved Fe^{3+}. The $Fe(H_2O)_6^{3+}$ was found to be the most active soluble iron complex form in the activation of $S_2O_8^{2-}$. The pH effect in FH/$S_2O_8^{2-}$ system was quite expected, as the rate constant decreased as the solution pH increased from pH 3.2 to 7.8. However, the pH value has no significant effect on the 4tBP degradation in AK/$S_2O_8^{2-}$ system. Only heterogeneous reaction may occur in AK or FH suspensions, as no significant leaching of iron ions was detected even in acidic conditions. The surprising trend in AK/$S_2O_8^{2-}$ system may be explained by the higher isoelectric point/point-of-zero charge (9.6 − 10) of this solid, which leads to a higher sorption capacity on oxide surfaces. Favorable electrostatic interactions between protonated 4tBP and negatively charged $S_2O_8^{2-}$ species adsorbed on positively charged oxide surfaces of AK may improve the heterogeneous oxidation mechanism.

4tBP degradation was mainly due to the $SO_4^{\bullet -}$ in IOs/$S_2O_8^{2-}$ system, while $SO_4^{\bullet -}$ and $HO_2^{\bullet}$ both had great contribution in the 4tBP degradation in Fe^{3+}/$S_2O_8^{2-}$ system. In the presence of chloride ions, 4tBP degradation efficiency was significantly decreased due to the trapping of $SO_4^{\bullet -}$ by Cl^-. The addition of carbonates at pH 8.2 completely inhibited the 4tBP degradation.

These results are very promising and may have strong implications in the treatment of contaminated waters and soils, especially where Fe^{3+} species are naturally occurring.

Acknowledgements

The authors gratefully acknowledge financial support from China Scholarship Council for. Yanlin Wu to study at the Blaise Pascal University in Clermont-Ferrand, France.

This work was supported by the National Natural Science Foundation of China (NSFC 21077031), China Postdoctoral Science Foundation (2016M591710) and Foundation of State Key Laboratory of Pollution Control and Resource Reuse (Tongji University) (PCRRY15005). This work was also supported by the "Federation des Recherches en Environnement" through the CPER "Environnement" founded by the "Région Auvergne," the French government and FEDER from European community. We thank Pr. J-F. Boily (Umea University) for providing akaganeite sample.

References

[1] R.L. Johnson, P.G. Tratnyek, R.O.B. Johnson, Persulfate persistence under thermal activation conditions, Environ. Sci. Technol., 42 (2008) 9350-9356.
[2] R.H. Waldemer, P.G. Tratnyek, R.L. Johnson, J.T. Nurmi, Oxidation of chlorinated ethenes by heat-activated persulfate: Kinetics and products, Environ. Sci. Technol., 41 (2007) 1010-1015.
[3] Y.-H. Guan, J. Ma, X.-C. Li, J.-Y. Fang, L.-W. Chen, Influence of pH on the formation of sulfate and hydroxyl radicals in the UV/peroxymonosulfate system, Environ. Sci. Technol., 45 (2011) 9308-9314.
[4] Y.-q. Gao, N.-y. Gao, Y. Deng, Y.-q. Yang, Y. Ma, Ultraviolet (UV) light-activated persulfate oxidation of sulfamethazine in water, Chem. Eng. J., 195-196 (2012) 248-253.
[5] T.K. Lau, W. Chu, N.J.D. Graham, The aqueous degradation of butylated hydroxyanisole by UV/$S_2O_8^{2-}$: Study of reaction mechanisms via dimerization and mineralization, Environ. Sci. Technol., 41 (2007) 613-619.
[6] Y.-T. Lin, C. Liang, J.-H. Chen, Feasibility study of ultraviolet activated persulfate oxidation of phenol, Chemosphere, 82 (2011) 1168-1172.
[7] G.P. Anipsitakis, D.D. Dionysiou, Radical generation by the interaction of transition metals with common oxidants, Environ. Sci. Technol., 38 (2004) 3705-3712.
[8] X. Jiang, Y. Wu, P. Wang, H. Li, W. Dong, Degradation of bisphenol A in aqueous solution by persulfate activated with ferrous ion, Environ. Sci. Poll. Res., 20 (2013) 4947-4953.
[9] C. Liang, Y.-y. Guo, Mass transfer and chemical oxidation of naphthalene particles with zerovalent iron activated persulfate, Environ. Sci. Technol., 44 (2010) 8203-8208.
[10] R.E. Huie, C.L. Clifton, P. Neta, Electron transfer reaction rates and equilibria of the carbonate and sulfate radical anions, Int. J. Radiat. Appl. Instrum. C Radiat. Phys. Chem., 38 (1991) 477-481.
[11] P.F. Killian, C.J. Bruell, C. Liang, M.C. Marley, Iron (II) ativated persulfate oxidation of MGP contaminated soil, Soil Sediment. Contam., 16 (2007) 523-537.
[12] Y. Deng, C.M. Ezyske, Sulfate radical-advanced oxidation process (SR-AOP) for simultaneous removal of refractory organic contaminants and ammonia in landfill leachate, Water Res., 45 (2011) 6189-6194.
[13] S.-X. Li, D. Wei, N.-K. Mak, Z. Cai, X.-R. Xu, H.-B. Li, Y. Jiang, Degradation of diphenylamine by persulfate: Performance optimization, kinetics and mechanism, J. Hazard. Mater., 164 (2009) 26-31.
[14] M. Ahmad, A.L. Teel, R.J. Watts, Persulfate activation by subsurface minerals, J. Contam. Hydrol., 115 (2010) 34-45.
[15] C. Liang, C.J. Bruell, M.C. Marley, K.L. Sperry, Persulfate oxidation for in situ remediation of TCE. I. Activated by ferrous ion with and without a persulfate-thiosulfate redox couple, Chemosphere, 55 (2004) 1213-1223.
[16] D.A. House, Kinetics and mechanism of oxidations by peroxydisulfate, Chem. Rev., 62 (1962) 185-203.
[17] R. Woods, I.M. Kolthoff, E.J. Meehan, Arsenic(IV) as an intermediate in the induced oxidation of arsenic(III) by the iron(II) persulfate reaction and the photoreduction of iron(III). II. Presence of oxygen, J. Am. Chem. Soc., 85 (1963) 3334-3337.
[18] J. De Laat, H. Gallard, Catalytic decomposition of hydrogen peroxide by Fe(III) in homogeneous aqueous solution: mechanism and kinetic modeling, Environ. Sci. Technol., 33 (1999) 2726-2732.
[19] J.J. Pignatello, Dark and photoassisted iron(3+)-catalyzed degradation of chlorophenoxy herbicides by hydrogen peroxide, Environ. Sci. Technol., 26 (1992) 944-951.

[20] J.-y. Zhao, Y.-b. Zhang, X. Quan, Z. Ya-zhi, Sodium peroxydisulfate activation by heat and Fe(II) for the degradation of 4-CP, Environ. Sci., 31 (2010) 1233-1238.
[21] A.L. Teel, M. Ahmad, R.J. Watts, Persulfate activation by naturally occurring trace minerals, J. Hazard. Mater., 196 (2011) 153-159.
[22] M. Usman, P. Faure, K. Hanna, M. Abdelmoula, C. Ruby, Application of magnetite catalyzed chemical oxidation (Fenton-like and persulfate) for the remediation of oil hydrocarbon contamination, Fuel, 96 (2012) 270-276.
[23] X. Duan, H. Sun, J. Kang, Y. Wang, S. Indrawirawan, S. Wang, Insights into heterogeneous catalysis of persulfate activation on dimensional-structured nanocarbons, ACS Catalysis, 5 (2015) 4629-4636.
[24] G. Fang, C. Liu, J. Gao, D.D. Dionysiou, D. Zhou, Manipulation of persistent free radicals in biochar to activate persulfate for contaminant degradation, Environ. Sci. Technol., 49 (2015) 5645-5653.
[25] Y. Lei, C.-S. Chen, Y.-J. Tu, Y.-H. Huang, H. Zhang, Heterogeneous degradation of organic pollutants by persulfate activated by CuO-Fe_3O_4: Mechanism, stability, and effects of pH and bicarbonate ions, Environ. Sci. Technol., 49 (2015) 6838-6845.
[26] Y. Li, L.-D. Liu, L. Liu, Y. Liu, H.-W. Zhang, X. Han, Efficient oxidation of phenol by persulfate using manganite as a catalyst, J. Mol. Catal. A: Chem., 411 (2016) 264-271.
[27] T. Zhang, Y. Chen, Y. Wang, J. Le Roux, Y. Yang, J.-P. Croué, Efficient peroxydisulfate activation process not relying on sulfate radical generation for water pollutant degradation, Environ. Sci. Technol., 48 (2014) 5868-5875.
[28] Y.-H. Jo, S.-H. Hong, T.-J. Park, S.-H. Do, The synthesized and thermally modified Mn-Ca-FeOOH composite in persulfate system: Its role to discolor methylene blue, Appl. Surf. Sci., 301 (2014) 576-583.
[29] H. Liu, T.A. Bruton, F.M. Doyle, D.L. Sedlak, In situ chemical oxidation of contaminated groundwater by persulfate: Decomposition by Fe(III)- and Mn(IV)-containing oxides and aquifer materials, Environ. Sci. Technol., 48 (2014) 10330-10336.
[30] T. Zhang, H. Zhu, J.-P. Croué, Production of sulfate radical from peroxymonosulfate induced by a magnetically separable $CuFe_2O_4$ spinel in Water: Efficiency, stability, and mechanism, Environ. Sci. Technol., 47 (2013) 2784-2791.
[31] H. Liu, T.A. Bruton, W. Li, J.V. Buren, C. Prasse, F.M. Doyle, D.L. Sedlak, Oxidation of benzene by persulfate in the presence of Fe(III)- and Mn(IV)-containing oxides: Stoichiometric efficiency and transformation products, Environ. Sci. Technol., 50 (2016) 890-898.
[32] C.F. Baes, R.E. Mesmer, The hydrolysis of Cations, 1976.
[33] A.V. Barse, T. Chakrabarti, T.K. Ghosh, A.K. Pal, S.B. Jadhao, One-tenth dose of LC50 of 4-tert-butylphenol causes endocrine disruption and metabolic changes in Cyprinus carpio, Pestic. Biochem. Physiol., 86 (2006) 172-179.
[34] S. Myllymaki, T. Haavisto, M. Vainio, J. Toppari, J. Paranko, In vitro effects of diethylstilbestrol, genistein, 4-tert-butylphenol, and 4-tert-octylphenol on steroidogenic activity of isolated immature rat ovarian follicles, Toxicol. Appl. Pharmacol., 204 (2005) 69-80.
[35] Z. Liu, Y. Kanjo, S. Mizutani, Removal mechanisms for endocrine disrupting compounds (EDCs) in wastewater treatment-physical means, biodegradation, and chemical advanced oxidation: A review. Sci. Total. Environ., 407(2009) 731–748.
[36] C.G. Campbell, S.E.Borglin, F.B. Green, A. Grason, E.Wozei, W.T. Stringfellow, Biologically directed environmental monitoring, fate, and transport of estrogenic endocrine disrupting compounds in water: a review. Chemosphere, 65(2006) 1265–1280.

[37] E. Lipctnska-Kochany, G. Sprah, S. Harms, Influence of some groundwater and surface waters constituents on the degradation of 4-chlorophenol by the Fenton reaction. Chemosphere, 30 (1995) 9-20.
[38] K. Hanna, Sorption of two aromatic acids onto iron oxides: Experimental study and modeling, J. Colloid Interface Sci., 309 (2007) 419-428.
[39] K. Hanna, C. Carteret, Sorption of 1-hydroxy-2-naphthoic acid to goethite, lepidocrocite and ferrihydrite: Batch experiments and infrared study, Chemosphere, 70 (2007) 178-186.
[40] P.A. Kozin, J.F.O. Boily, Proton binding and ion exchange at the akaganeite/water interface, J. Phys. Chem. C, 117 (2013) 6409-6419.
[41] A. Bianco, M. Passananti, H. Perroux, G. Voyard, C. Mouchel-Vallon, N. Chaumerliac, G. Mailhot, L. Deguillaume, M. Brigante, A better understanding of hydroxyl radical photochemical sources in cloud waters collected at the puy de Dôme station: experimental vs. modeled formation rates, Atmos. Chem. Phys., 15 (2015) 13923-13955.
[42] R. Matta, K. Hanna, S. Chiron, Fenton-like oxidation of 2,4,6-trinitrotoluene using different iron minerals, Sci. Total Environ., 385 (2007) 242-251.
[43] W.P. Kwan, B.M. Voelker, Rates of hydroxyl radical generation and organic compound oxidation in mineral-catalyzed Fenton-like systems, Environ. Sci. Technol., 37 (2003) 1150-1158.
[44] R. Marsac, S. Martin, J.-F. Boily, K. Hanna, Oxolinic acid binding at goethite and akaganéite surfaces: Experimental study and modeling, Environ. Sci. Technol., 50 (2016) 660-668.
[45] W.J. McElroy, S.J. Waygood, Kinetics of the reactions of the SO_4^- radical with $SO_4^{-\bullet}$ $S_2O_8^{2-}$ H_2O and Fe^{2+}, in: G. Restelli, G. Angeletti (Eds.) Physico-Chemical Behaviour of Atmospheric Pollutants: Air Pollution Research Reports, Springer Netherlands, Dordrecht, 1990, pp. 251-256.
[46] X.Y. Yu, Z.C. Bao, J.R. Barker, Free radical reactions involving $Cl^\bullet$, $Cl_2^{-\bullet}$, and $SO_4^{-\bullet}$ in the 248 nm photolysis of aqueous solutions containing $S_2O_8^{2-}$ and Cl, J. Phys. Chem. A, 108 (2004) 295-308.
[47] H. Mestankova, G. Mailhot, J.-F. Pilichowski, J. Krysa, J. Jirkovsky, M. Bolte, Mineralisation of Monuron photoinduced by Fe(III) in aqueous solution, Chemosphere, 57 (2004) 1307-1315.
[48] G.V. Buxton, C.L. Greenstock, W.P. Helman, A.B. Ross, Critical review of rate constants for reactions of hydrated electrons, hydrogen atoms and hydroxyl radicals ($^\bullet OH/^\bullet O^-$) in aqueous solution, J. Phys. Chem. Ref. Data, 17 (1988) 513-886.
[49] P. Neta, R.E. Huie, A.B. Ross, Rate constants for reactions of inorganic radicals in aqueous solution, J. Phys. Chem. Ref. Data, 17 (1988) 1027-1284.
[50] Y. Wu, A. Bianco, M. Brigante, W. Dong, P. de Sainte-Claire, K. Hanna, G. Mailhot, Sulfate radical photogeneration using Fe-EDDS: Influence of critical parameters and naturally occurring scavengers, Environ. Sci. Technol., 49 (2015) 14343-14349.
[51] J. Hu, W. Fan, W. Ye, C. Huang, X. Qiu, Insights into the photosensitivity activity of BiOCl under visible light irradiation, Appl. Catal., B, 158-159 (2014) 182-189.
[52] M. Stylidi, D.I. Kondarides, X.E. Verykios, Visible light-induced photocatalytic degradation of Acid Orange 7 in aqueous TiO_2 suspensions, Appl. Catal., B, 47 (2004) 189-201.
[53] S.S. Lin, M.D. Gurol, Catalytic decomposition of hydrogen peroxide on iron oxide: Kinetics, mechanism, and implications, Environ. Sci. Technol., 32 (1998) 1417-1423.
[54] G.G. Jayson, B.J. Parsons, A.J. Swallow, Some simple, highly reactive, inorganic chlorine derivatives in aqueous solution. Their formation using pulses of radiation and their role in the mechanism of the Fricke dosimeter, J. Chem. Soc., Faraday Trans. 1, 69 (1973) 1597-1607.
[55] V. Nagarajan, R.W. Fessenden, Flash photolysis of transient radicals. 1. X2- with X = Cl, Br, I, and

SCN, J. Phys. Chem., 89 (1985) 2330-2335.
[56] M. Brigante, M. Minella, G. Mailhot, V. Maurino, C. Minero, D. Vione, Formation and reactivity of the dichloride radical ($Cl_2^{\bullet-}$) in surface waters: A modelling approach, Chemosphere, 95 (2014) 464-469.
[57] C. Busset, P. Mazellier, M. Sarakha, J. De Laat, Photochemical generation of carbonate radicals and their reactivity with phenol, J. Photochem. Photobiol., A 185 (2007) 127–132.
[58] M.H. Nie, Y. Yang, Z.J. Zhang, C.X. Yan, X.Q. Wang, H.Q. Li, W.B. Dong, Degradation of chloramphenicol by thermally activated persulfate in aqueous solution, Chem. Eng. J. 246 (2014) 373–382.
[59] C. Tan, N. Gao, Y. Deng, Y. Zhang, M. Sui, J. Deng, S. Zhou, Degradation of antipyrine by UV, UV/H2O2 and UV/PS, J. Hazard. Mater., 260 (2013) 1008– 1016.

Figures

Figure 1: 4tBP degradation in the presence of iron oxhydroxides (IO) and $S_2O_8^{2-}$ ([IO] = 1g L^{-1}; [$S_2O_8^{2-}$] = 1 mM; [4tBP] = 50 µM; pH = 4.7). The line represents the exponential decay of experimental data.

Figure 2: Effect of solid loading (in terms of exposed surface area per volume unit) on the 4tBP degradation rate constant ([$S_2O_8^{2-}$] = 1 mM; [4tBP] = 50 µM; pH = 4.7)

Figure 3: Effect of pH on the 4tBP degradation rate constant ([$S_2O_8^{2-}$] = 1 mM; [4tBP] = 50 µM). AK and FH were tested at the same surface area, *i.e.* 120 m^2 L^{-1}, corresponding to 0.49 g $L^{-1}$for FH and 0.50 g L^{-1} for AK.

Figure 4: Effect of pH on the 4tBP degradation rate constant in Fe^{3+}/ $S_2O_8^{2-}$ system ([Fe^{3+}] = 11.2 mM; [$S_2O_8^{2-}$] = 1 mM; [4tBP] = 50 µM).

Figure 5: Effect of Fe^{3+} concentration on the 4tBP degradation rate constant ([$S_2O_8^{2-}$] = 1 mM; [4tBP] = 50 µM; pH = 2.4)

Figure 6: Effect of 2-Pr, t-BuOH and BQ on the degradation of 4tBP after 3 hours reaction ([Fe^{3+}] = 5.6 mM or [IO] = 0.5 g L^{-1}; [$S_2O_8^{2-}$] = 1 mM; [2-Pr] = [t-BuOH] = [BQ] = 50 mM; [4tBP] = 50 µM; pH = 2.4)

Figure 7: Effect of Cl^- concentration on the 4tBP degradation in the presence of 0.5 g L^{-1} of Akaganeite (filled symbols) and Ferrihydrite (empty symbols) with [$S_2O_8^{2-}$] = 1 mM. [4tBP] = 50 µM; pH = 4.7. Data are fitted with an exponential decay curve.

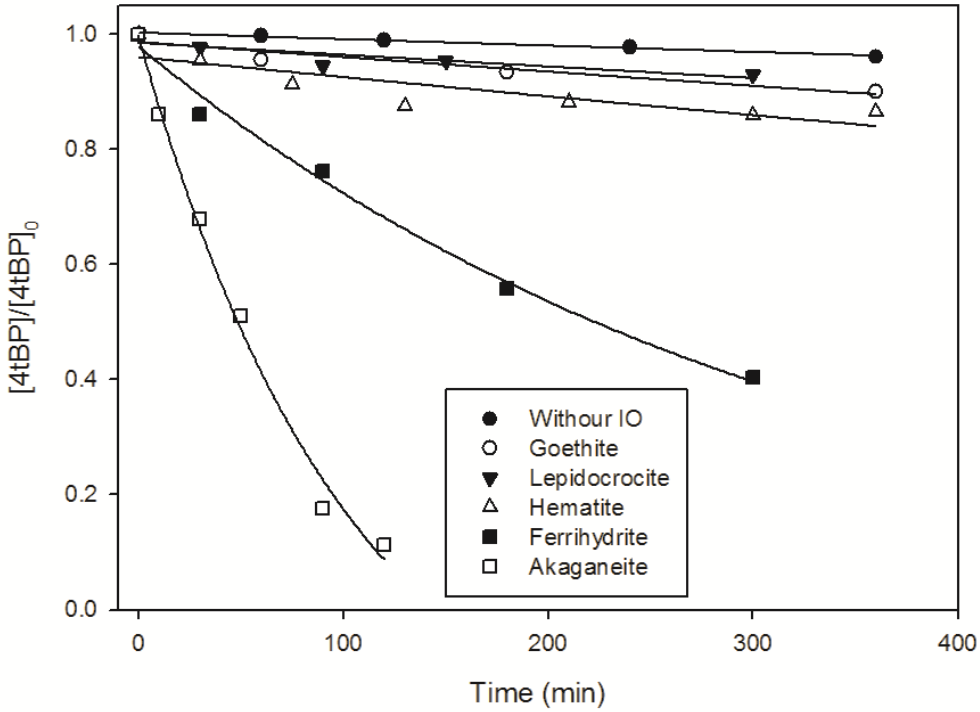

Figure 1

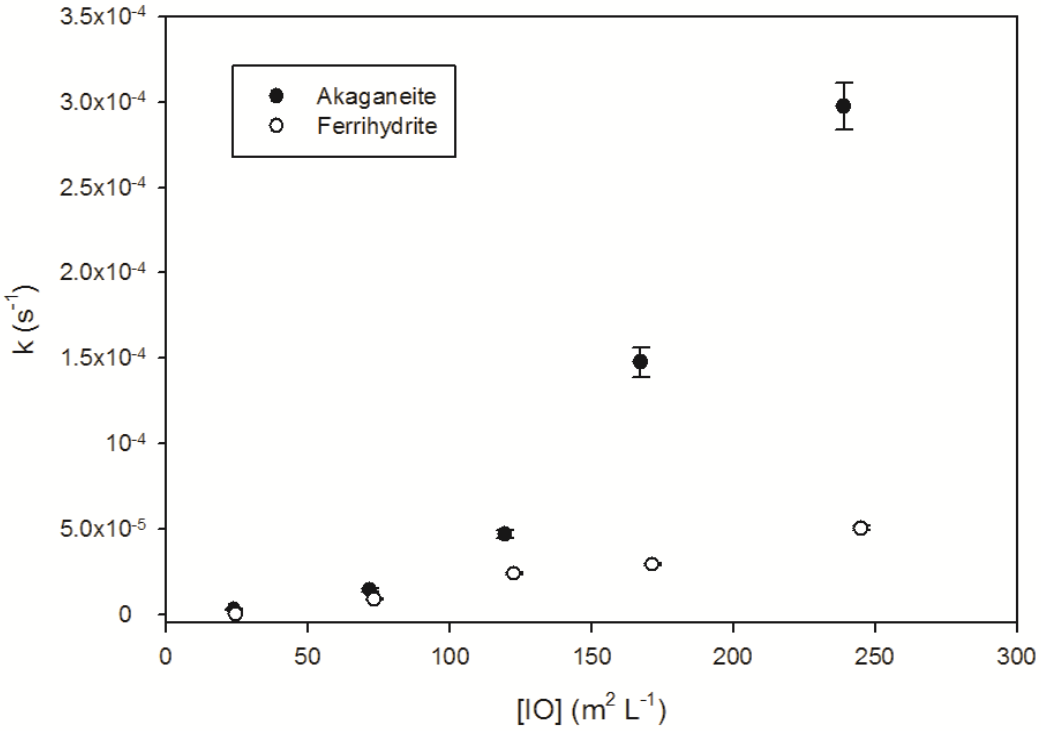

Figure 2

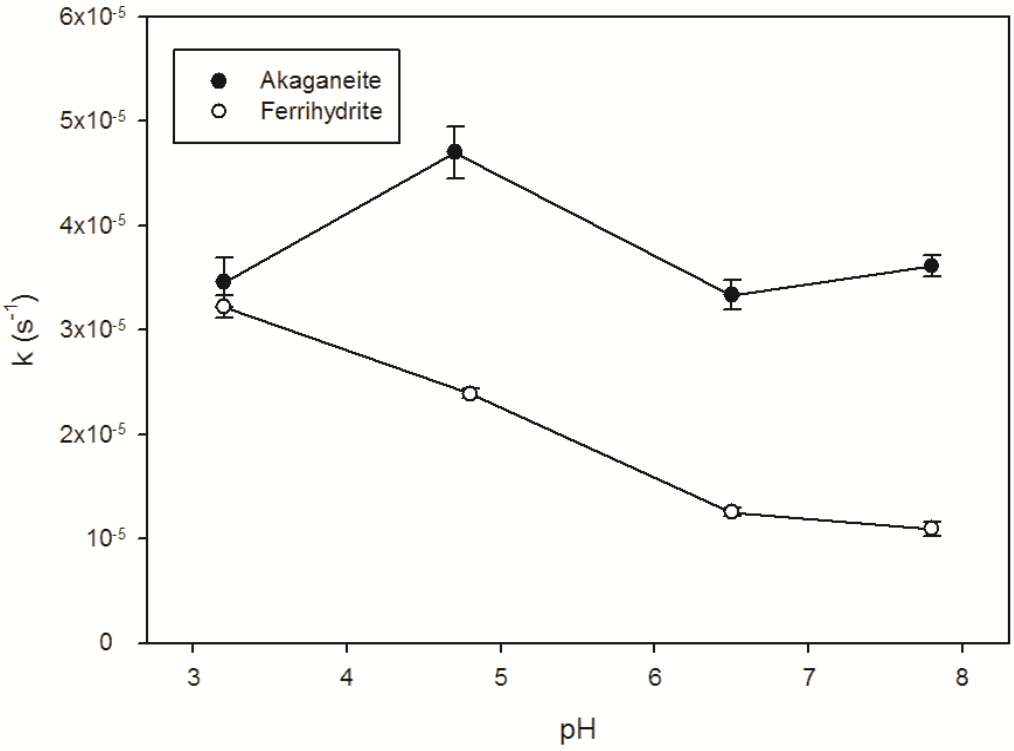

Figure 3

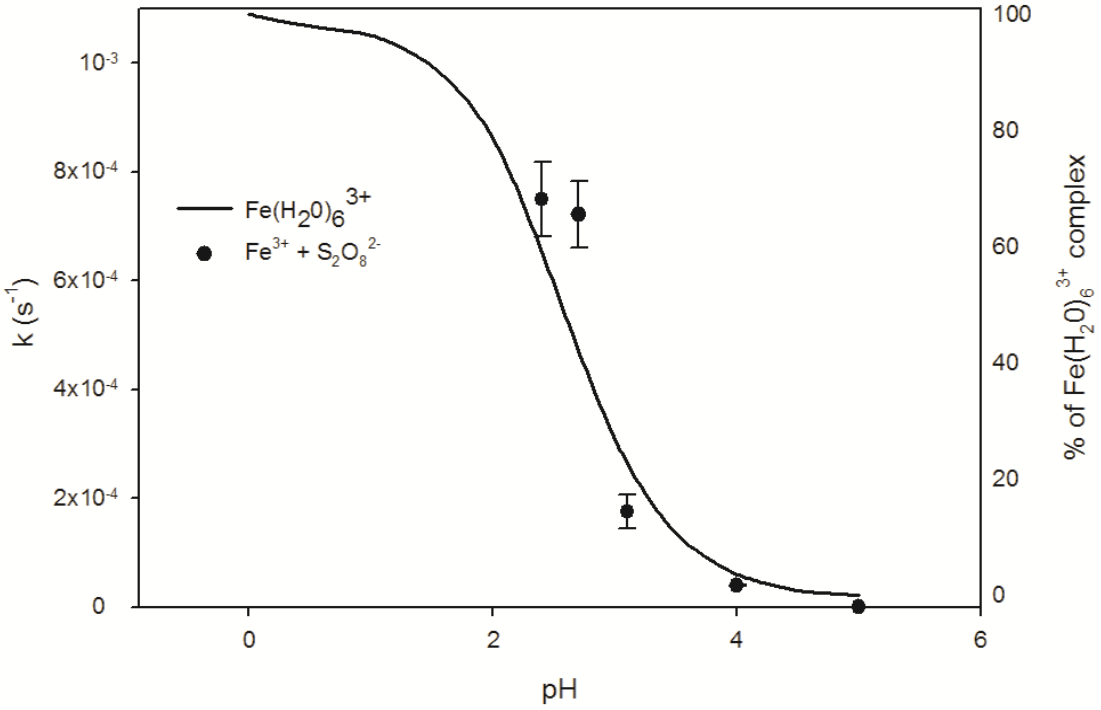

Figure 4

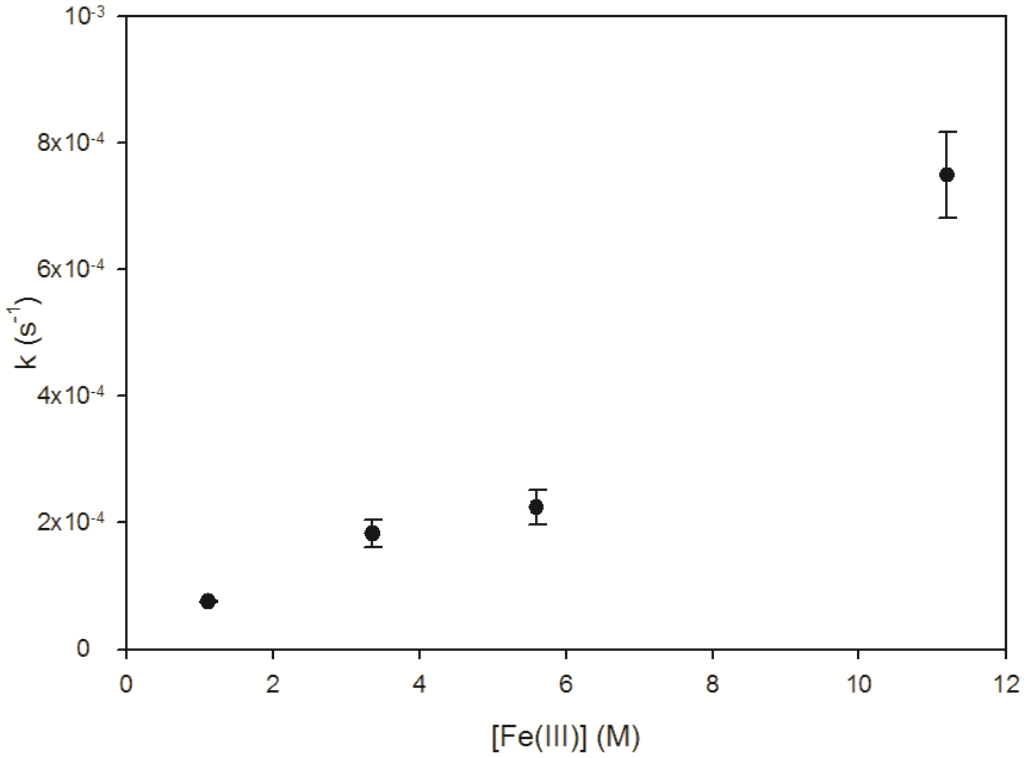

Figure 5

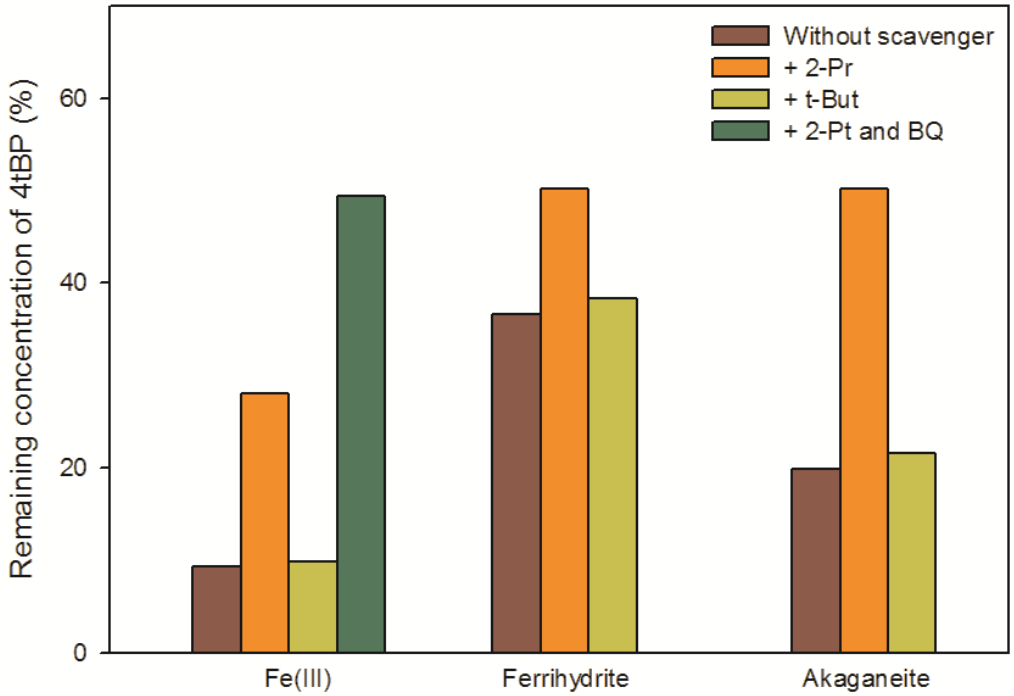

Figure 6

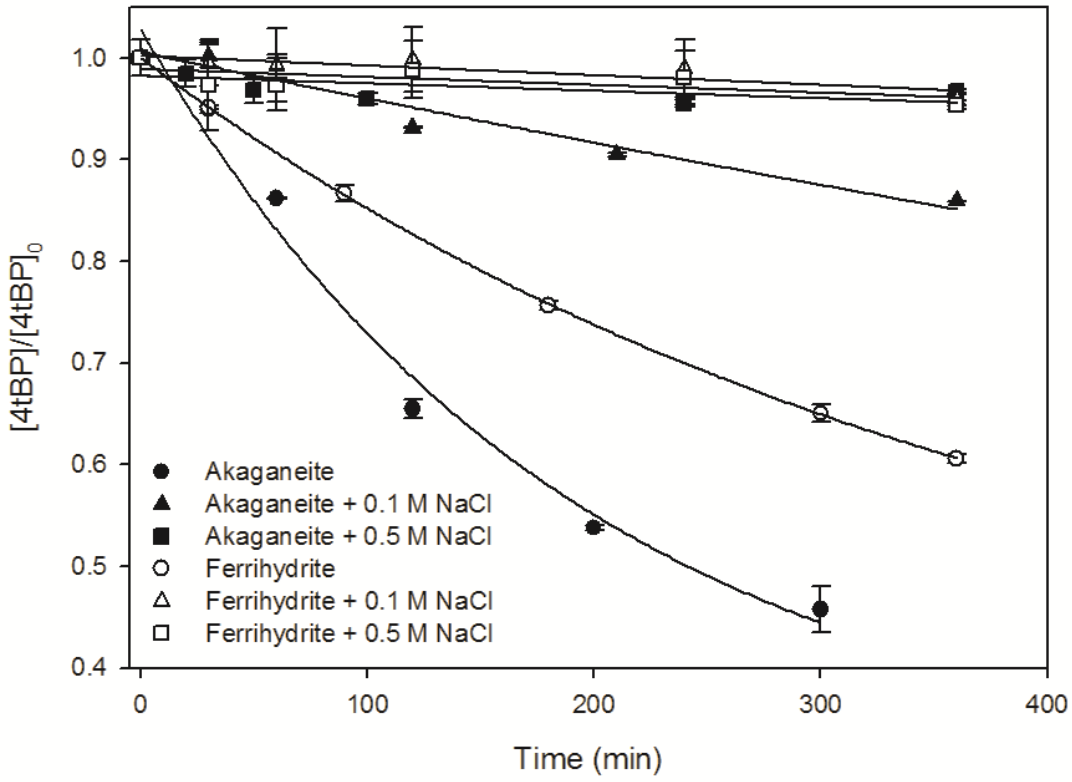

Figure 7

Table 1. Physicochemical parameters of the investigated iron oxhydroxides

Mineral	**BET surface area (m^2 g^{-1})**	**Shape : Average particle size**	**PZC**
Goethite α-FeOOH	49	acicular : 50-60 nm in width and 200-300 nm in length	9.1
Ferrihydrite $Fe_2(OH)_6$	245	Spherical : 5-6 nm in diameter	8.2
Lepidocrocite γ-FeOOH	59	acicular: 2.5-6.3 nm in width and 11-50 nm in length	7.9
Hematite Fe_2O_3	16	Spherical : 80-90 nm in diameter	8.1
Akaganeite β-FeOOH	239	acicular : 2.5-6.3 nm in width and 11-50 nm in length	9.5